

# Evolution of Four Formulae Derived Over Five Decades to Predict Temporal Scour at Circular Pier



Buddhadev Nandi, Krishanu Sasmal, and Subhasish Das

## 1 Introduction

The interaction of stream flow and a vertical bridge supporting structure which are creating an obstruction to the flow generates erosion of the sediment bed due to complicated three-dimensional flow separation [1]. The transverse resistivity of the soil supporting the foundation decreases substantially with increasing scour depth, resulting in horizontal deflection of the foundation head. The most significant human aspects are: the insufficiency of hydrological data to base flood magnitude estimations for design purposes; the *absence of reliable techniques for estimating scour at bridge piers*; as well as an inability to predict the impact and accumulation of debris against the bridge structure [2]. In front of such obstructions, the flow velocity is less and on the side of the obstruction, the flow velocity increase which reduces the bed shear stress and the sediment lifted by the action of the horseshoe vortex leads the erosion. Most of the widely used empirical formulas for estimating scour depth under clear water equilibrium (CWE) conditions are derived under conditions of extremely long flow periods. Bridge pier footings designed keeping CWE condition, scour depths can offer significantly higher values than when the flow lasts for a shorter period of time. Smaller scour depths can be attained for a limited time to the peak value of the planned flood hydrograph, thus minimizing the total construction costs. As a result, it is critical to investigate the temporal variation of CWE scour. However, time-dependent studies on the local scouring phenomenon are few.

To determine the maximum depth of scour at bridge piers, several computational and laboratory investigations were conducted. But based on these concepts, bridge pier design may not be cost-effective. Thus, the concept of temporal scour depth ( $S_{dt}$ ) is established. The  $S_{dt}$  is a crucial requirement for safe and cost-effective construction of bridge piers [3]. Due to the gradually increasing scientific interest in evaluating

---

B. Nandi (✉) · K. Sasmal · S. Das  
School of Water Resources Engineering, Jadavpur University, Kolkata, West Bengal, India  
e-mail: [buddhadevnandi95@gmail.com](mailto:buddhadevnandi95@gmail.com)

$S_{dt}$ , a number of prediction formulae are available [3–9]. Several researchers [10–12] studied the evolution of  $S_{dt}$  using well-established computation models.

In the present study, to predict  $S_{dt}$  at a circular pier in CWE conditions, four formulae are selected among those that have been derived over five decades. Such four selected formulae are taken from (i) Shen et al. [4], (ii) Melville and Chiew [3], (iii) NCHRP [12] and (iv) Franzetti et al. [9]. These four formulae are compared with well-established  $S_{dt}$  experimental data developed by Yanmaz and Altinbilek [13] to verify the accuracy of individual formulae. In addition, several statistical influencing factors are analyzed to achieve the goal.

## 2 Four Formulae and Experimental Procedure

Several computational and laboratory studies were performed to determine the  $S_{dt}$  in CW condition. The reliability of four previously established promising  $S_{dt}$  formulae, given below, are tested in this work using 16 literature data from [13] which were conducted in CW conditions with homogeneous bed material.

Shen et al. [4] obtained a formula for scour depth as a function of time by fitting the data from [14] to an exponential function, Eq. 1. The formula was created for circular pier and is predicated on a constrained set of flow and sediment parameters. The same was adopted by NCHRP [12]. Here,  $P_d$  is pier diameter,  $F$  is Froude number,  $d_w$  is depth of flow,  $V$  is velocity of the flow, and  $t$  is time. Parameters,  $J$  and  $R$  are dependent upon  $d_w$ ,  $P_d$ ,  $V$ ,  $t$ , and  $F$  and are determined from the relations given in [12].

Melville and Chiew [3] have collected 84 laboratory sets and developed Eq. 2. This Eq. 2 was used in [8, 11, 12]. Here,  $V_c$  is the critical velocity,  $V_{*c}$  is critical shear velocity,  $d_{50}$  is median sediment diameter, and  $T$  is reference time. Now,  $V_{*c}$  and  $T$  can be determined using other formulae given in [3]. The accuracy of Formula 2 was improved by adjusting the parameters and substituting the maximum scour depth formula with Eq. 2 given in [12], known as S/M formula (Eq. 3). Here,  $K_1$  is arbitrary constant equaling  $-0.04$ . Here,  $T$  is determined using other formulae as proposed in [12].

Franzetti et al. [9] proposed a new predictor (Eq. 4) using laboratory data collected from 30 sources and 328 experiments, to evaluate time-dependent and greatest  $S_{dt}$  at circular pier in CW conditions. Five dimensionless parameters such as pier slenderness, flow strength, sediment coarseness, and  $t$  were considered. Here,  $c = 2.57$  (constant),  $S$  is sediment relative density, and  $\sigma$  is sediment geometric standard deviation. All related parameter functions are calculated using other formulae given in [9].

$$\frac{S_{dt}}{P_d} = 2.5F^{0.4}\{1 - \exp(JR^2)\} \quad (1)$$

**Table 1** Summary of data with necessary experimental range

References	$d_w/P_d$	$V/V_c$	$P_d/d_{50}$	$\Delta$	$\sigma$	$F$
Yanmaz and Altinbilek [13]	1.27–3.51	0.75–0.951	43.93–79.76	1.63–1.64	1.13–1.28	0.28–0.29

$$\frac{S_{dt}}{S_e} = \exp \left\{ -0.03 \left| \frac{V_c}{V} \ln \left( \frac{t}{T} \right) \right|^{1.6} \right\} \tag{2}$$

$$\frac{S_{dt}}{S_e} = \exp \left\{ K_1 \left| \frac{V_c}{V} \ln \left( \frac{t}{T} \right) \right|^{1.6} \right\} \tag{3}$$

$$\frac{S_{dt}}{P_d} = c f_1 \left( \frac{d_w}{P_d} \right) f_2 \left( \frac{P_d}{d_{50}} \right) f_3(\sigma) f_4 \left( \frac{V}{V_c} \right) f_5 \left( \frac{tV}{P_d(S-1)^{0.5}} \right) \tag{4}$$

To determine how the  $S_{dt}$  changes, [9] conducted laboratory experiments using single circular bridge pier perspex models with homogeneous bed materials and CW conditions in a  $90 \times 67 \text{ cm}^2$  flume with a 5-m long approach arm. The  $P_d$  values of 6.7, 5.7, and 4.7 cm were used for two different uniform bed materials having specific densities of 2691.1 and 2680.9  $\text{kg/m}^3$ ,  $d_{50}$  of 1.07 and 0.84 mm. The angle of attack remained constant as  $V$  increased. A sketch of 16 selected datasets by [13] is shown in Table 1.

### 3 Functional Frameworks

Scour depth develops over time and is determined by water flow, sediment properties ( $\sigma$ ,  $\rho_s$ ,  $d_{50}$ ,  $V_c$ ), geometry of the obstacle on the bed profile and time. So, the functional relationship can be written as (Eq. 5). Here, the flow parameters are  $\rho$ ,  $\nu$ ,  $g$ ,  $d_w$ ,  $V$ ;  $\gamma$  is a correction factor for bed form;  $\alpha$  is shape correction factor for obstruction. The functional framework for the selected four literature formulae with their non-dimensional parameters is listed in Table 2.

$$S_{dt} = f^n(\rho_f, \rho_s, \nu, \gamma, g, d_w, V, \sigma, d_{50}, V_c, \alpha, \beta, P_d, t, T) \tag{5}$$

### 4 Performance of Existing Formulae

In the current study, four previously invented formulae were evaluated for verifying their performance using literature data for CW conditions and the homogeneous bed material. However, due to the homogeneity of the current data, the  $V/V_c$  value

**Table 2** Parameter for construction of functional framework of four literature formulae

Serial No	Researchers	Functions
1	Shen et al. [4]	$S_{dt}/P_d = f(F, P_d/d_w, d_w, V_t/d_w)$
2	Melville and Chiew [3]	$S_{dt}/S_e = f(V/V_c, \ln(t/T))$
3	NCHRP [12]	$S_{dt}/S_e = f(V/V_c, \ln(t/T))$
4	Franzetti et al. [9]	$S_{dt}/P_d = f(V/V_c, P_d/d_{50}, \sigma, d_w/P_d, \Delta, (tV/P_d \Delta^{0.5}))$

is found smaller than unity, which clearly reflects the CW experimental condition. The accuracy of four formulae dedicatedly created to estimate  $S_{dt}$  was graphically validated, as well as the consideration of several statistical influencing parameters. In Figs. 1, 2, 3, 4 the solid lines are the perfect agreement (PA) lines and dashed lines show  $\pm 20\%$  deviation from individual PA lines between the observed and predicted normalized  $S_{dt}$ .

In Figs. 1 and 4, the X axis represents the observed  $S_{dt}$  normalized with  $P_d$  and the Y axis represents the computed  $S_{dt}$  normalized with  $P_d$ . In Figs. 2 and 3, the X axes represent the observed  $S_{dt}$  normalized with  $S_e$  and Y axes represent the computed  $S_{dt}$  normalized with  $S_e$ . The numerical formulas for  $S_{dt}$  estimation used in [3, 9, 12], and [4] are shown in Figs. 1–4 and collected data from literature [13] are plotted as computed versus measured normalized  $S_{dt}$ .

When compared to the observed and computed data by [9], 82% of the literature data falls under the  $\pm 20\%$  error line, as seen in Fig. 1. When all 16 datasets were

**Fig. 1** Comparison using Eq. 4 [9]

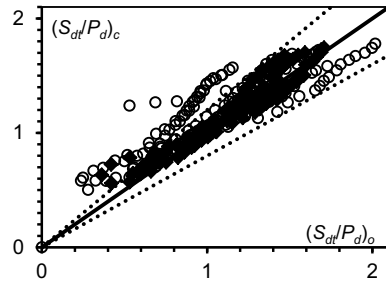


**Fig. 2** Comparison using Eq. 2 [3]

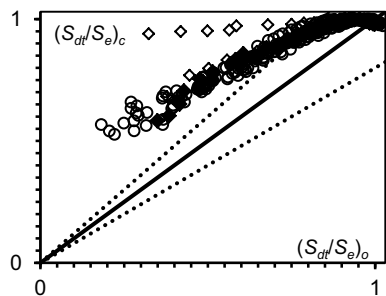


**Fig. 3** Comparison using Eq. 3 [12]

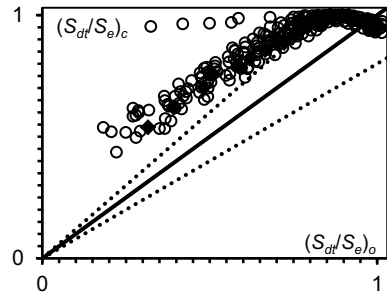
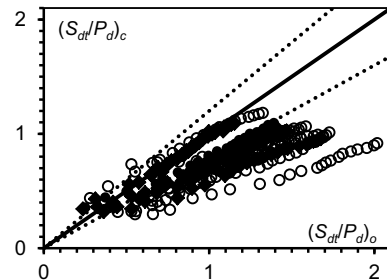


**Fig. 4** Comparison using Eq. 1 [4]



compared, three of them fared poorly. The figure shows that no data series is outside the -20% error line, but three hardly few data series points exceed the +20% error band, which is within the maximum bound limit set in [9]. Under prediction of scour depth is conservative and should be avoided in real-world applications; nevertheless, excessive over prediction is equally troublesome for the application engineer when building such bridge piers because it is not economic in engineering terms. However, a higher value for the structural design can be used to produce a higher factor of safety. Both the issue reported in [9], the formula needs to be multiplied by 1.6, i.e., the constant  $c = 4.1$  instead of 2.57, for estimating upper-bound scour value.

When computed versus measured normalized scour depth are presented in comparison to each other, 48% of the data from the literature are outside of the  $\pm 20\%$  error line. Although all data series initially overestimate the temporal scour depth, at a later stage the computed value is within the error band, as can be seen in Fig. 2, nearly 50% of data points lie outside the 20% error band. As we all know, the upper bound limit is what the field or application engineer works with, however significantly over calculated data results in uneconomical designs for construction. Therefore, calculating the  $S_e$  is helpful, but from the temporal perspective, it is rather difficult.

Here, 54% of the data from the literature are outside the  $\pm 20\%$  error line when computed versus measured normalized  $S_{dt}$  are compared to one another. Even though all data series initially overestimate the temporal scour depth at a later stage, as can be shown in Fig. 3, approximately half of the data points fall below the 20% error

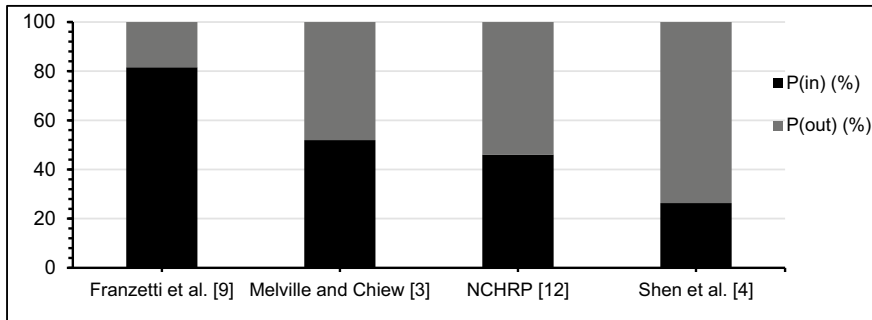


**Fig. 5** Percentages in [P(in)] and out [P(out)] considering all 16 datasets

zone. As we all know, the field or application engineer works with the upper bound limit, but drastically over estimated data leads to unsustainable construction designs.

Similar to this, when comparing computed versus measured average scour depth for Shen et al.'s [4] formula presented in Fig. 4., 26% of data from the literature falls within the  $\pm 20\%$  error line. About three-fourths of them, are outside the error band and, of those, nearly all of those data points are outside the  $-20\%$  error band, which makes them useless for designing hydraulic structures like bridges because application engineers occasionally use overestimated values that are within the upper bound limit.

Figure 5 shows the numerical formula for scour depth estimation by [3, 9, 12 and 4] and the data which had been selected from the literature were plotted as computed versus measured normalized scour depth. From the figure, it can be seen that 82% of the literature data falls inside the  $\pm 20\%$  error line when compared to the observed and computed data by [9]. Similarly, 52%, 46%, and 26% of data from the literature fall under the  $\pm 20\%$  error line when compared with the formulae in [3, 4] and [12].

## 5 Sensitivity Analysis

A variety of statistical parameters are also used to evaluate the correctness of the literature formulae. Here, 10 statistical parameters are used to indicate the data accuracy namely Correlation Coefficient (CC), RMSE, Coefficient of Determination ( $R^2$ ), Nash Sutcliffe Efficiency (NSE), Sum of Squared Errors (SSE), MAE, MAPE, NRMSE, Kling-Gupta efficiency (KGE), and Index agreement (IA) shown in Table 3. Compare the predictor performance in this study among four literature formulae in terms of several statistical influencing factors.

The Pearson product-moment CC, sometimes known as Pearson's CC and  $R^2$  equalling the squared value of Pearson's CC, is the most well-known indicator of dependency between two quantities. The highest CC and  $R^2$  are observed for [3] and

**Table 3** Sensitivity analysis of selected four literature formulae

Authors	CC	RMSE	R <sup>2</sup>	NSE	SSE	MAE	MAPE	NRMSE	KGE	IA	P <sup>out</sup> (%)
Franzetti <i>et al.</i> [9]	0.91	0.18	0.82	0.76	9.6	0.14	0.14	0.16	0.81	0.93	18
Melville and Chiew [3]	0.94	0.19	0.88	0.18	10.83	0.16	0.16	0.26	0.53	0.75	48
NCHRP [12]	0.88	0.19	0.78	0.14	11.43	0.17	0.17	0.27	0.55	0.74	54
Shen <i>et al.</i> [4]	0.72	0.41	0.52	-0.32	52.17	0.34	0.34	0.37	0.41	0.66	74

the lowest values are observed in the case of [4], However, [9] has CC and R<sup>2</sup> values of 0.91 and 0.82 respectively, the second highest among all.

It is simpler to compare models with various scales according to the NRMSE, which links the RMSE to the observed range of the variable. The absolute error is the difference between the computed value and the observed value, represented as an absolute number. The mean absolute error is the average of the absolute differences between computed and real observations, where each difference is given equal weight (MSE). The least squares approach for generating regression coefficients minimizes the SSE, which indicates the error is not eliminated by the regression line. The most popular method of measuring forecasting error is the MAPE, presumably because the units of the variable are scaled to percentages and are therefore simpler to comprehend. In the instance of [9], the non-beneficial criteria such as NRMSE, RMSE, SSE, MAE, and MAPE have lower values, whereas, in the case of [4], they have the highest value.

The IA standardizes the measurement of the model prediction error, which ranges from 0 to 1. The quality of fit measure provides a diagnostically interesting decomposition of the NSE. Taylor skill score links the models’ correlation coefficient and standard deviations. For Franzetti *et al.* [9] formula, the remaining beneficial criteria have the highest value, while Shen *et al.* [4] formula has the lowest value.

To evaluate each formula [3, 4, 9, 12], the beneficial criteria in Table 3 are arranged in decreasing order and the non-benefit criteria are arranged in increasing order. P<sub>out</sub> values (%) are also arranged in increasing order to evaluate all four formulas. It is noticeable that Eq. (3) [9] performs better than the other formulas as the value of all beneficial criteria is higher and non-beneficial terms are lower in the case of Eq. (3) [9] as shown in Table 3.

## 6 Conclusions

Several researchers carried out studies to estimate temporal scour depth,  $S_{dt}$ . The current study considers four formulas derived over the last six decades. Due to the limited data set collected from the laboratory experiments, this study tries to select the best one for predicting the  $S_{dt}$ . Ten different statistical performance metrics, such as CC, RMSE,  $R^2$ , NSE, SSE, MAE, MAPE, NRMSE, KGE, and IA and the proportion of data points outside of the 20% error zone are used to evaluate the performance of the formulae.

The parameters included in this study to measure the computed  $S_{dt}$  using four such formulae are flow factors, bed sediment properties, pier geometry and time. The effectiveness of the scour function is quantified as a percentage of the experimental data point for which the normalized computed scour depth differs from the measured one by more than 20% using 16 experimental data from the literature.

Franzetti et al. [9] formula performed better on four-fifths of the data points. Half of the data points outperformed in the case of both Melville and Chiew [3] and NCHRP [12] formulae and for Shen et al. [4] formula, three-fourths of the data set outperformed. It is observed that hardly a few beneficial criteria (CC,  $R^2$ ) are greater in the case of Melville and Chiew [3] formula, However, Franzetti et al. [9] formula also has good agreement with respect to CC and  $R^2$ . For all other beneficial and non-beneficial criteria such as RMSE, NSE, SSE, MAE, MAPE, NRMSE, KGE, and IA, Franzetti et al. [9] formula performed well in comparison with other formulae.

## References

1. Das S, Das R, Mazumdar A (2013) Circulation characteristics of horseshoe vortex in the scour region around circular piers. *Water. Sci. Eng.* 6(1):59–77
2. Zhang G, Liu Y, Liu J, Lan S, Yang J (2022) Causes and statistical characteristics of bridge failures: A review, *J Traffic Transp Eng* (2022)
3. Melville BW, Chiew YM (1999) Time scale for local scour at bridge piers. *J Hydraul Eng* 125(1):59–65
4. Shen HW, Schneider VR, Karaki S (1966) Mechanics of local scour: supplement, methods of reducing scour, Doctoral dissertation. Colorado State University, Libraries
5. Sumer BM, Christiansen N, Fredsøe J (1993) Influence of cross-section on wave scour around piles. *J Waterway Port Coast Ocean Eng.* 119(5):477–495
6. Oliveto G, Hager WH (2002) Temporal evolution of clear-water pier and abutment scour. *J Hydraul Eng* 128(9):811–820
7. Lança RM, Fael CS, Maia RJ, Pêgo JP, Cardoso AH (2013) Clear-water scour at comparatively large cylindrical piers. *J Hydraul Eng* 139(11):1117–1125
8. Choi SU, Choi B (2016) Prediction of time-dependent local scour around bridge piers. *Water Environ J* 30(1–2):14–21
9. Franzetti S, Radice A, Rebai D, Ballio F (2022) Clear water scour at circular Piers: A new formula fitting laboratory data with less than 25% deviation. *J Hydraul Eng* 148(10):1–13
10. Mia MF, Nago H (2003) Design method of time-dependent local scour at circular bridge pier. *J Hydraul Eng* 129(6):420–427
11. Simarro G, Fael CMS, Cardoso AH (2011) Estimating equilibrium scour depth at cylindrical piers in experimental studies. *J Hydraul Eng* 137(9):1089–1093

12. Sheppard DM, Demir H, Melville B (2011) Scour at wide piers and long skewed piers, NCHRP Rep. No. 682. (2011) Washington, DC: Transportation Research Board
13. Yanmaz AM, Altinbilek HDGA (1991) Study of time-dependent local scour around bridge piers. *J Hydraul Eng* 117(10):1247–1268
14. Chabert J, Engeldinger P (1956) Étude des affouillements autour des piles de ponts, Technical Rep. [In French.] Chatou, France: Laboratoire National d'Hydraulique